6475

Revision 4

Thermodynamic properties of natural melilites

LYUBOV P. OGORODOVA[1,*], **YULIYA D. GRITSENKO**[1,2],
MARINA F. VIGASINA[1], **ANDREY Yu. BYCHKOV**[1], **DMITRY A. KSENOFONTOV**[1],
LYUBOV V. MELCHAKOVA[1]

[1] Geological Faculty, M.V. Lomonosov Moscow State University, Leninskie Gory, Moscow, 119234, Russia
[2] Fersman Mineralogical Museum RAS
Russia, Moscow, 117071, Leninskiy prospect 18 - 2

ABSTRACT

In the present study, four samples of natural melilites were characterized using electron microprobe analysis, powder X-ray diffraction, FTIR and Raman spectroscopy, and their thermodynamic properties were measured with a high-temperature heat-flux Tian-Calvet microcalorimeter. The enthalpies of formation from the elements were determined to be: -3795.8 ± 4.1 kJ/mol for $Ca_{1.8}Na_{0.2}(Mg_{0.7}Al_{0.2}Fe^{2+}_{0.1})Si_2O_7$, -3753.1 ± 5.2 kJ/mol for $Ca_{1.6}Na_{0.4}(Mg_{0.5}Al_{0.4}Fe^{2+}_{0.1})Si_2O_7$, -3735.3 ± 3.7 kJ/mol for $Ca_{1.6}Na_{0.4}(Mg_{0.4}Al_{0.4}Fe^{2+}_{0.2})Si_2O_7$, and -3929.2 ± 3.8 kJ/mol for $Ca_2(Mg_{0.4}Al_{0.6})[Si_{1.4}Al_{0.6}O_7]$. Using the obtained formation enthalpies and estimated entropies, the standard Gibbs free energies of formation of these melilites were calculated. Finally, the enthalpies of the formation of the end members of the isomorphic åkermanite-gehlenite and åkermanite – alumoåkermanite series were derived. Obtained in this work thermodynamic properties of melilites of different composition can be used for quantitative modeling of formation conditions of these minerals in geological and technological processes.

Keywords: Melilite, åkermanite, gehlenite, alumoåkermanite, thermochemistry, enthalpy of formation, entropy, Gibbs free energy, Calvet microcalorimetry.

INTRODUCTION

Melilites are a group of rock-forming sorosilicates, including solid solutions with several end members. The general formula of melilites has the form $A_2B(T_2O_7)$, where A = Ca, Na, Ba; B = Al, Mg, Fe^{2+}, Zn, Be, B; T = Al, Si, B. There are eleven minerals in the melilite group: gehlenite, åkermanite, alumoåkermanite, hardystonite, gugiaite, okayamalite, barylite, andremeyerite, leucophanite, jeffreyite and meliphanite (Fleischer's glossary of mineral species 2014). Their structure is tetragonal with the space group $P\bar{4}2_1m$ (D^3_{2d}), $Z = 2$. Melilites typically occur in high-calcium ultrabasic alkaline igneous rocks: in some rocks they are the main rock-forming minerals, while in others (contact-metasomatic rocks, calcareous skarns) they are less often found. In addition, melilites are constituents of some calcium- and aluminium-rich inclusions in chondritic meteorites.

Gehlenite $Ca_2Al[SiAlO_7]$ and åkermanite $Ca_2Mg[Si_2O_7]$ are the most common melilites. Available data on melilites from volcanic and plutonic rocks show that their chemical compositions reflect the degrees of evolution of melts from which the formation of these rocks occurred during crystallization differentiation (Egorov 1969; Wiedenmann 2009). Åkermanite is a typical mineral of primitive rocks, melilitolites, olivinites, kugdites, and uncompahgrites. Alumoåkermanite $CaNaAl[Si_2O_7]$ and åkermanite, appreciably enriched in both Na and Al, are characteristic minerals of nephelinites, turiyaites, and okayites, i.e. feldspathoid rocks, crystallized from residual melts. Gehlenite is also found in high-temperature calcareous skarns in association with dolomite, calcite, spinel, vesuvian, phlogopite, grossular, apatite, etc.

X-ray diffraction and Raman spectroscopy studies of synthesized melilites (mainly åkermanite and gehlenite) were carried out previously (Charlu et al. 1981; Sharma et al. 1988; Bouhifd et al.

2002; Najafinezhad et al. 2017); results for natural melilites from different localities are presented in RRUFF Database (RRUFF project). The natural alumoåkermanite was studied by Wiedenmann et al. (2009). FTIR absorption spectra of natural melilite samples are given in Chukanov (2014).

Practical interest in the physicochemical properties of melilites lies in the fact that melilites of the isomorphic åkermanite-gehlenite series are typical minerals of blast furnace slags. The regularities of change in the chemical and mineralogical composition of slags determine the criteria by which the technological parameters of melting regime are established. The presence of these minerals at specific stages of melting provides an opportunity to monitor and optimize the melting process. Domain slags are characterized by a relatively constant chemical composition and are environmentally safe. Materials based on metallurgical melilite containing slags can be used in house building, as the basis of road surfaces, as a sintering additive and the main component in the production of heat-resistant ceramic products (Mal'kova 2006).

The availability of reliable thermodynamic parameters of these minerals is necessary for thermodynamic modeling of melilite formation in nature, for determining stability fields in multicomponent slag-forming mixtures, and for optimizing the synthesis parameters of akermanite bioceramics, e.g., used for bone tissues. There are available thermodynamic data on synthesized end members of the isomorphic series åkermanite - gehlenite. Weller and Kelly (1963), Hemingway and Robie (1984), and Hemingway et al. (1986) measured the low-temperature heat capacities of these substances using adiabatic calorimeters and calculated the values of their standard entropies. Data on the enthalpies of formation of åkermanite and gehlenite are summarized in Table 1. The enthalpies of formation of åkermanite from the oxides and the elements were determined using acid solution calorimetry (Neuvonen 1952, Barany 1963) and high temperature melt solution calorimetry (Charlu et al. 1981; Brousse et al. 1984). The enthalpy of formation of gehlenite was obtained by melt solution calorimetry (Charlu et al. 1981). The calorimetric data, the results calculated from *P*-*T* equilibria studies, and the values estimated using different theoretical models are given in reference books (Naumov et al. 1971; Robie et al. 1978, Robie and Hemingway 1995) and articles (Berman 1988; Holland and Powell 1990, 1998, 2011; Ottonello et al. 2013).

The purpose of this study was to determine the standard enthalpies of formation of natural melilites using calorimetry and to derive their Gibbs free energies of formation based on the measured formation enthalpies and estimated entropies.

SAMPLES AND METHODS

Four samples of natural melilites were chosen for this study.

Sample I was taken from the pegmatoid zone of Phlogopite mine of Kovdor carbonatite massif (Kola Peninsula, Russia). It is represented by large (up to 30 cm) monomineral melilite aggregates surrounded by diopside, phlogopite and fluorapatite. Melilite has a gray color with a bluish tinge and bright glass shine.

Sample II was derived from the alkaline ultrabasic massif of Turi Mys (Kandalaksha Gulf, Karelia, Russia). It consists of semitransparent grayish melilite crystals in association with nepheline and lepidomelane.

Sample III was selected from nepheline-diopside-garnet-melilite pegmatite bodies of the ultramafic carbonatite of Odihincha massif (Polar Siberia, Krasnoyarsk Territory, Russia). Melilite is presented in the form of large (up to 20 cm) prismatic semitransparent brownish-gray crystals, substituted by an aggregate of cebollite, juanite and hydrogrossular at the edges. The central parts of the crystals, which are free of the alteration products, were used in this study.

Sample IV was found in the skarn locality of the Vesuvianovaya gorka in the Kudabek region (Azerbaijan). It is massive, dense small- and medium-grained aggregates of isometric grains of colorless melilite in association with carbonate and apatite.

Samples I and III were taken from the personal collection of one of the authors (Gritsenko Yu.D.), while samples II and IV were from the collections of the Fersman Mineralogical Museum Russian Academy of Sciences (No. 90274 and 41299, respectively).

Chemical analysis was done using an electron microprobe analyzer (EMPA) Camebax-microbeam (France) with an energy-dispersive Si (Li) detector and an INCA Energy Oxford analysis system. The accelerating voltage used was 20 kV, and beam current was- 30 nA.

X-ray diffraction was carried out using a powder diffractometer «STOE-STADI MP» (Germany) equipped with a curved Ge(111) monochromator which gives strictly monochromatic $CoK_{\alpha1}$ radiation (λ = 1.78897 Å). Data were collected in a regime of sequential overlapping of scanned regions using a linear position-sensitive detector with a 2θ coverage of 5° and a channel width of 0.02°. Unit-cell parameters of melilites were derived from the obtained XRD data using software packages $WinX^{Pow}$ ($WinX^{Pow}$ Software STOE & CIE GmbH 2002) and XPowINDEX (which includes Werner`s TREOR, Visser`s ITO and Louer`s DICVOL).

Raman spectroscopy was performed with a Raman microspectrometer EnSpector R532 (Russia) which includes a OLYMPUS CX41 microscope equipped with a 40x objective and a monochromator with a dispersion grating of 1800 lines/mm. The wavelength of the diode laser radiation was 532 nm, the output power of the beam was 30 mW, the spectral resolution was 6 cm^{-1}, and the diameter of the focal spot was about 15 μm. The spectra were obtained in the range from 100 to 4000 cm^{-1} on powdered melilite samples; the exposition time was 1 s and the signal averaging was done using 50 expositions. The instrument was calibrated against the Raman line of silicon with a frequency of 520.5 cm^{-1}.

FTIR spectroscopy was carried out using a Fourier spectrometer FSM-1201 (Russia) in the range from 400 to 4000 cm^{-1} with an accuracy of ± 2 cm^{-1} in the mode of transmittance. The samples were prepared in the form of a suspension in the vaseline oil.

Drop-solution calorimetric measurements of melilites were carried out with a high-temperature heat-flux Tian-Calvet microcalorimeter "Setaram" (France). Molten $2PbO \cdot B_2O_3$ was used as the solvent; it was prepared by melting stoichiometric amounts of lead oxide and boric acid at 1073 K. The experiments were performed by the "drop" method: samples with a mass of 1.5-6.5 (± 2.10^{-3}) mg were dropped from room temperature into the $2PbO \cdot B_2O_3$ melt in the calorimeter at 973 K; the measured thermal effect included the heat content of the sample and its enthalpy of solution [$\Delta H = H^0$ (973 K) $-H^0$ (298.15 K) + $\Delta_{sol}H^0$ (973 K)). The large ratio of the melt solvent to dissolved sample can be referred to an infinitely dilute solution with the mixing enthalpy close to zero when 6 - 8 samples were dropped into the melt solvent weighing 30-35 g. The samples dissolved readily and gave a complete reaction within 30-50 min before a steady baseline was restored. Calibration of the microcalorimeter was performed using a reference substance – platinum, and the data of its enthalpy increments were taken from Robie and Hemingway (1995). Using the obtained heats of drop solution, the enthalpies of formation were calculated based on a thermochemical cycle including the dissolution of melilite and its constituent oxides. Details of high-temperature oxide-melt calorimetry were described by Navrotsky (2014), and this technique has been used for thermochemical studies of a variety of mineral phases and synthetic materials including silicates (e.g., Xu et al. 1999, 2000, 2001; Balmer et al. 2001; Ogorodova et al. 2003, 2012, 2014, 2015).

The electron microprobe analyzer used is located in the Fersman Mineralogical Museum, Russian Academy of Sciences, and all other instruments are at the Geological Faculty of M.V. Lomonosov Moscow State University.

RESULTS AND DISCUSSION

Sample characterization

Electron microprobe analysis (EMPA). EMPA data for the minerals studied are shown in Table 2. Their chemical formulas calculated on a 7-oxigen basis are:

$(Ca_{1.8}Na_{0.2})(Mg_{0.7}Al_{0.2}Fe^{2+}_{0.1})Si_2O_7$ (I),

$(Ca_{1.6}Na_{0.4})(Mg_{0.5}Al_{0.4}Fe^{2+}_{0.1})Si_2O_7$ (II),

$(Ca_{1.6}Na_{0.4})(Mg_{0.4}Al_{0.4}Fe^{2+}_{0.2})Si_2O_7$ (III),

$Ca_{2.0}(Mg_{0.4}Al_{0.6})[Si_{1.4}Al_{0.6}O_7]$ (IV).

The studied melilites belong to two isomorphic series: gehlenite - åkermanite and åkermanite - alumoåkermanite (Fig. 1). Sample (IV) is related to the mineral form of gehlenite; the content of gehlenite is ~60%; the åkermanite content is ~39%; and the alumoåkermanite content is ~1%. This sample is an intermediate member of the isomorphic series of gehlenite - åkermanite, where the isomorphism is described by the scheme: $Al^{3+} + Al^{3+} \leftrightarrow Mg^{2+} + Si^{4+}$. Samples (I - III) are associated with åkermanite with a sequential increase in the alumoåkermanite content from 20 to 40% while gehlenite is absent. The Na_2O content varies from 2.75 to 4.88 wt%, and the SiO_2 content is essentially constant (44.14 - 44.76 wt%). The isomorphism is expressed by the scheme: $Ca^{2+} + Mg^{2+} \leftrightarrow Na^{+} + Al^{3+}$ (Wiedenmann et al. 2009). The replacement of Mg^{2+} by Fe^{2+} (up to 4 wt% FeO) is more characteristic of aluminous melilites such as those from Oldonho Lengai, Tanzania (Wiedenmann et al. 2009).

Powder X-ray diffraction. XRD patterns of natural melilites are shown in Fig 2a. The patterns of samples I and II correspond to those of Kovdor åkermanite (Kola Peninsula, Russia) (RRUFF project, card R061085); the pattern of sample III is close to that of alumoåkermanite from Oldonho Lengai (Tanzania) (Wiedenmann, et.al., 2009); the pattern of sample IV agrees with XRD data of gehlenite from Monzoni, (Tyrol, Italy) (RRUFF project, card R060841). The differences in the XRD patterns of studied melilites are highlighted in Figs. 2b and 2c. The peaks for gehlenite (sample IV) are shifted towards larger 2Θ angles compared with those of åkermanite - alumoåkermanite series (samples I-III). The differences among the patterns of samples I-III mainly lie in their different peak intensities, perhaps reflecting different degrees of crystallinity. Melilites containing alumoåkermanite (samples I-III) are characterized by the appearance of two additional peaks, (012) and (112), in the region of 42-47° and the peak (411) at about 61° (Wiedenmann et.al. 2009) for alumoåkermanite. Their appearance is probably due to the incorporation of Na^{+} into the melilite structure**.** The obtained unit-cell parameters, unit-cell volumes and molar volumes of melilites are listed in Table 3. Unit-cell parameters of the åkermanite - alumoåkermanite series vary with increasing the ålumoåkermanite component: *a* decreases markedly, whereas *c* increases to a lesser extent. Gehlenite is characterized by the smallest *a* and the largest *c*.

Raman spectroscopy. The obtained spectra of natural melilites are shown in Fig. 3. According to the Raman study of synthetic åkermanite and gehlenite by Sharma et al. (1988), samples (I-III) can be attributed to åkermanites, and sample (IV) to gehlenite. Two spectral regions can be distinguished in the spectra of melilitites. The high-frequency region (1000-600 cm^{-1}) includes Raman bands corresponding predominantly to the stretching vibrations of the bonds in the disilicate units Si_2O_7 (samples I-III) and $(Si, Al)_2O_7$ (sample IV) and tetrahedral groups AlO_4 and MgO_4. When Al occupies the Si position in the twin tetrahedron, the number of spectral components in this range increases from 6 (samples I-III) to 10 (sample IV). The strong intensities observed in this range are from: 1) the scattering lines with maxima at about 916, 923, 924 and 909 cm^{-1}, which are associated with the valence symmetric vibrations of SiO_3 groups from Si_2O_7 dimers; 2) the lines with maxima at about 666, 664, 664 and 618 cm^{-1} corresponding to the valence symmetric vibrations of (Si,Al)-O-Si bridges; and 3) the lines with maxima at about 625, 631, 631 and 618 cm^{-1}, which correspond to the symmetric stretching vibrations of the bonds in the tetrahedral groups MgO_4 (samples I-III) and AlO_4 (sample IV). In the low-frequency region (600 - 200 cm^{-1}), there are scattering lines associated with the deformation vibrations of various types and translational vibrations of the large structural units and cations. Specifically, the weak lines within the frequency range from 528 to 434 cm^{-1} arise from deformation oscillations of O-(Si,Al)-O in $(Si,Al)O_3$, the lines with frequencies from 310 to 236 cm^{-1} are associated with torsional vibrations of $(Si,Al)O_3$, and the lines with even lower frequencies may be attributed to translational vibrations of cations and lattice modes (Sharma et al. 1988).

FTIR spectroscopy . IR absorption spectra of the studied melilites are presented in Fig. 4. The samples with similar chemical compositions (samples I-III) exhibit similar spectral profiles. The observed increase in the number of bands in the range from 1017 to 810 cm^{-1} in the sample (IV) spectrum may be due to the presence of Al at the Si position in $(Si, Al)_2O_7$.

The assignment of absorption bands in IR spectra is analogous to the assignment of scattering lines in Raman spectra. The IR spectra of samples (I) and (IV) coincide to the spectra of melilites of similar compositions (Chukanov 2014), the spectrum of sample (I) is close to that of åkermanite (Sid 27), and sample (IV) has a spectrum similar to that of gehlenite (Sid 18).

In summary, our EMPA, XRD and Raman/FTIR spectroscopic studies have shown that the samples are single phases and are suitable for calorimetric determination of the thermodynamic properties of melilites.

Standard enthalpies of formation of natural melilites

The enthalpies of formation of melilites from the elements were calculated from their measured heats of drop solution (Table 4) using reactions (1-4) and equations (5, 6).

For sample (I):

$$1.8\ CaO + 0.1\ Na_2O + 0.7\ MgO + 0.1\ Al_2O_3 + 0.05\ Fe_2O_3 + 2\ SiO_2 \rightarrow$$

$$\rightarrow (Ca_{1.8}Na_{0.2})(Mg_{0.7}Al_{0.2}Fe^{2+}_{0.1})Si_2O_7 + 0.025O_2, \qquad (1)$$

Sample (II):

$$1.6\ CaO + 0.2Na_2O + 0.5\ MgO + 0.2\ Al_2O_3 + 0.05\ Fe_2O_3 + 2\ SiO_2 \rightarrow$$

$$\rightarrow (Ca_{1.6}Na_{0.4})(Mg_{0.5}Al_{0.4}Fe^{2+}_{0.1})Si_2O_7 + 0.025O_2, \qquad (2)$$

Sample (III):

$$1.6\ CaO + 0.2Na_2O + 0.4\ MgO + 0.2\ Al_2O_3 + 0.1\ Fe_2O_3 + 2\ SiO_2 \rightarrow$$

$$\rightarrow (Ca_{1.6}Na_{0.4})(Mg_{0.4}Al_{0.4}Fe^{2+}_{0.2})Si_2O_7 + 0.05O_2, \qquad (3)$$

Sample (IV):

$$2\ CaO + 0.4\ MgO + 0.6\ Al_2O_3 + 1.4\ SiO_2 = Ca_2(Mg_{0.4}Al_{0.6})[Si_{1.4}Al_{0.6}O_7], \qquad (4)$$

$$\Delta_{r(1\text{-}4)}H^0(298.15\ \text{K}) = \Sigma\ \nu_i\Delta H\text{ox}_i - \Delta H\text{melilite} - \nu\Delta H\text{O}_2, \qquad (5)$$

$$\Delta H_f^0(298.15\ \text{K})\text{melilite} = \Delta_{r(1\text{-}4)}H^0(298.15\ \text{K}) + \Sigma\ \nu_i\Delta H_f^0(298.15\ \text{K})\text{ox}_i, \qquad (6)$$

where ν is stoichiometric ratios of oxides and oxygen in the formation reaction of melilites; ΔHmelilite and $\Delta H\text{ox}_i$ $\{= [H^0(973\ \text{K}) - H^0(298.15\ \text{K}) + \Delta_{sol}H^0(973\ \text{K})]\}$ are drop-solution calorimetric data of natural melilites (Table 4) and constituent oxides (Table 5), respectively; $\Delta H\text{O}_2$ is heat content $[H^0(973\ \text{K}) - H^0(298.15\ \text{K})]$ of oxygen from Robie and Hemingway (1995); the values of $\Delta_f H^0{}_{el}(298.15\ \text{K})$ are the enthalpies of formation of oxides from the elements (Table 5). Note that since it was not possible to measure the heat of drop solution of FeO in molten lead borate (due to oxidation of Fe^{2+}), we assumed that the small amounts (0.1-0.2 formula units) of iron containing in the melilite minerals are in the trivalent form. The obtained values of $\Delta H_f^0(298.15\ \text{K})$ of melilites are listed in Table 6.

Gibbs free energies of formation of natural melilites

In order to calculate the Gibbs free energies of formation of melilites from the elements, we estimated their standard entropies, which are not available in the literature (Table 6). The values of $S^0(298.15\ \text{K})$ of synthetic melilites, obtained from low-temperature heat capacity measurements of åkermanite (Hemingway et al. 1986) and gehlenite (Hemingway and Robie 1984), were used for the $S^0(298.15\ \text{K})$ derivation of samples (I-III) and (IV), respectively. The calculation was based on the additive scheme of Holland (1989) on estimation of silicate entropies. Using the values of entropy contributions of oxides (S-V), where S and V are entropy and volume of oxides, and taking into account the coordination of the corresponding cations in the mineral structure (Holland 1989), we evaluated the standard entropies $S^0(298.15\ \text{K})$ of studied melilites. For example, for sample (I):

$$Ca_2MgSi_2O_7 + 0.1\ Na_2O + 0.1\ FeO + 0.1\ Al_2O_3 = Ca_{1.8}Na_{0.2}(Mg_{0.7}Al_{0.2}Fe^{2+}{}_{0.1})Si_2O_7 + 0.2\ CaO + + 0.3\ MgO, \qquad (7)$$

$S^0(298.15\ \text{K})$melilite = $S^0(298.15\ \text{K})$åkermanite+ $0.1(S\text{-}V)^{[8]}Na_2O + 0.1(S\text{-}V)^{[4]}FeO$ +

$$+ 0.1(S\text{-}V)^{[4]}\mathrm{Al_2O_3} - 0.2\,(S\text{-}V)^{[8]}\mathrm{CaO} - 0.3(S\text{-}V)^{[4]}\mathrm{MgO}, \qquad (8)$$

where the coordination numbers of cations in the melilite structure are given in square brackets, and the values (S-V) for oxides are taken from (Holland, 1989).

Using the derived S^0(298.15 K) and our measured ΔH_f^0(298.15 K) values, the standard Gibbs free energies of formation of these melilites from the elements were calculated (Table 6).

Thermodynamic properties of melilite end members

Using the obtained heats of drop solution of natural melilites in molten lead borate at 973 K, we calculated the enthalpies of formation of the end members of the isomorphic series of åkermanite-gehlenite and åkermanite-alumoåkermanite. To do this, the data for the studied melilites of the closest compositions were recalculated based on the molecular weights of melilite end members. The enthalpies of formation were calculated according to equations analogous to (1-6). The standard entropies were taken from Hemingway et al. (1986) for åkermanite and from Hemingway and Robie (1984) for gehlenite. The value of S^0(298.15 K) of aluminoåkermanite, not available in the literature, was estimated using equations analogous to (7, 8) for sample (I). The results are shown in Table 6.

Literature data on the enthalpy of formation (Table 1) for åkermanite $\mathrm{Ca_2Mg[Si_2O_7]}$ vary from -3860.441 to -3877.3 kJ/mol. Our value (-3853.9 ± 4.3 kJ/mol) agrees reasonably with this range and the ΔH_f^0(298.15 K) of a synthetic åkermanite, -3864.8 ± 2.0 kJ/mol (Robie and Hemingway 1995).

Literature data on ΔH_f^0(298.15 K) of gehlenite (Table 1) vary from -3969.54 to -3992.26 kJ/mol. The enthalpy of formation of synthetic gehlenite $\mathrm{Ca_2Al[SiAlO_7]}$ was previously determined to be -3978.98 kJ/mol (Charlu et al. 1981). The value obtained by us (-3982.4 ± 3.9 kJ/mol) falls within the limits of errors of the results of Charlu et al. (1981) and agrees with the value (-3985.0 ± 5.0 kJ/mol) given in Robie and Hemingway (1995).

The thermodynamic parameters of alumoåkermanite $CaNaAl[Si_2O_7]$ obtained in the present work are first determinations.

IMPLICATIONS

Natural melilite has a complex composition, but at present thermodynamic parameters are known only for pure end members of åkermanite - gehlenite solid solution. The new obtained experimental data on the enthalpy of formation for various natural melilites provides information for the development the thermodynamics of melilite solid solution. Such models of a solid solution make it possible to use melilite composition as an indicator of mineral formation processes conditions.

Experimental determination of the enthalpies and calculated values of Gibbs energies of formation of melilites allow quantitative thermodynamic modeling of phase equilibria in the system $(Mg,Ca)O\text{-}Al_2O_3\text{-}SiO_2\text{-}CO_2$ allow quantitative thermodynamic modeling of phase equilibria in the system $(Mg,Ca)O\text{-}Al_2O_3\text{-}SiO_2\text{-}CO_2$. The main reactions associated with the formation of contact-metasomatic rocks and calcareous skarns involve silicates and calcite:

$$2CaCO_3 + CaAl_2Si_2O_8 = Ca_2Al[SiAlO_7] + CaSiO_3 + 2CO_2\uparrow, \quad (9)$$

calcite (Cal) anortite (An) gehlenite (Gh) wollastonite (Wo)

$$CaCO_3 + CaMgSi_2O_6 = Ca_2MgSi_2O_7 + CO_2\uparrow. \quad (10)$$

calcite (Cal) diopside (Di) åkermanite (Åk)

Calculation of the phase equilibria using equations (9, 10) was carried out by HCh software (Shvarov 2008). The necessary thermodynamic parameters for other minerals included in reactions (9, 10) were taken from Holland and Powell (1998). The obtained results (Fig. 5, lines 1 and 2) are consistent with previous data of P-T equilibria involving akermanite (Walter 1963) and gehlenite (Hoschek 1974). An ideal åkermanite ─ gehlenite solid solution in equilibrium with calcite, diopside, anorthite, wollastonite and carbon dioxide was calculated (Fig. 5, line 3). The computed composition of melilite solid solution in the phase assemblage contains an åkermanite component ranging from 22 mol. % at 500°C to 29 mol. % at 800°C. As shown in

Fig. 5, at temperatures above about 600° C, the solid solution is more stable, as the pressure rises, than the pure end-member phases.

Stability boundaries of natural melilites (Fig. 5, lines 4, 5, 6 and 7) were calculated by equations (11, 12, 13, 14) with the addition of albite and fayalite using thermodynamic properties of melilites determined in this work.

$1.15CaCO_3 + 0.2NaAlSi_3O_8 + 0.7CaMgSi_2O_6 + 0.05Fe_2SiO_4 =$

calcite (Cal) albite (Ab) diopside (Di) fayalite (Fa)

$$= Ca_{1.8}Na_{0.2}(Mg_{0.7}Al_{0.2}Fe^{2+}_{0.1})Si_2O_7 + 0.05CaSiO_3 + 1.15CO_2\uparrow \tag{11}$$

(Sample I) wollastonite (Wo)

$1.35CaCO_3 + 0.4NaAlSi_3O_8 + 0.5CaMgSi_2O_6 + 0.05Fe_2SiO_4 =$

calcite (Cal) albite (Ab) diopside (Di) fayalite (Fa)

$$= Ca_{1.6}Na_{0.4}(Mg_{0.5}Al_{0.4}Fe^{2+}_{0.1})Si_2O_7 + 0.25CaSiO_3 + 1.35CO_2\uparrow \tag{12}$$

(Sample II) wollastonite (Wo)

$1.3CaCO_3 + 0.4NaAlSi_3O_8 + 0.4CaMgSi_2O_6 + 0.1Fe_2SiO_4 =$

calcite (Cal) albite (Ab) diopside (Di) fayalite (Fa)

$$= Ca_{1.6}Na_{0.4}(Mg_{0.4}Al_{0.4}Fe^{2+}_{0.2})Si_2O_7 + 0.1CaSiO_3 + 1.3CO_2\uparrow \tag{13}$$

(Sample III) wollastonite (Wo)

$1.6CaCO_3 + 0.6CaAl_2Si_2O_8 + 0.4CaMgSi_2O_6 =$

calcite (Cal) anortite (An) diopside (Di)

$$= Ca_2(Mg_{0.4}Al_{0.6})[Si_{1.4}Al_{0.6}O_7] + 0.6CaSiO_3 + 1.6CO_2\uparrow \tag{14}$$

(Sample IV) wollastonite (Wo)

Melilites can be formed during the reactions of calcite with silicates at temperatures above 400°C. The calculated lower temperature boundaries of stability for samples II and IV (Fig. 5, lines 4 and 5, respectively) are close to the stability boundary of the ideal åkermanite - gehlenite solid solution (Fig. 5, line 3). Samples I and III from carbonatites (Fig. 5, lines 7 and 6, respectively) are stable at lower temperatures due to the high amount of alumoåkermanite.

The thermodynamic characteristics of the members of the åkermanite-gehlenite series also allow us to perform thermodynamic modeling of the processes of crystallization of blast furnace slags. In industrial conditions, in the process of their cooling and crystallization, the physicochemical equilibrium is not reached, and therefore the determination of the mineral composition of the slag is impossible. Further practical use of this product of blast-furnace processes is determined not only by chemical, but also by its mineralogical composition.

REFERENCES CITED

Balmer, M.L., Su, Y., Xu, H., Bitten, E., McCready, D., and Navrotsky, A. (2001) Synthesis, structure determination, and aqueous durability of $Cs_2ZrSi_3O_9$. Journal of the American Ceramic Society, 84, 153-160.

Barany, R. (1963) Heats of formation of gehlenite and talc. U.S. Bureau of Mines Report Investigation, № 6251**,** 9 p.

Berman, R.G. (1988) Internally consistent thermodynamic data for minerals in the system Na_2O-K_2O-CaO-MgO-FeO-Fe_2O_3-Al_2O_3- SiO_2- TiO_2-H_2O-CO_2, Journal of Petrology, 29(2), 445-522.

Bouhift, M.A., Gruener, G., Mysen, B.O., and Richet, P. (2002) Premelting and calcium mobility in gehlenite ($Ca_2Al_2SiO_7$) and pseudowollastonite ($CaSiO_3$), Physics and Chemistry of Minerals, 29, 655-662.

Brousse, C., Newton, R.C., and Kleppa, O.J. (1984) Enthalpy of formation of forsterite, enstatite, akermanite, monticellite and merwinite at 1073 K determined by alkali borate solution calorimetry, Geochimica et Cosmochimica Acta, 48, 1081-1088.

Charlu, T.V., Newton, R.C., and Kleppa, O.J. (1981) Thermochemistry of synthetic $Ca_2Al_2SiO_7$ (gehlenite) – $Ca_2MgSi_2O_7$ (åkermanite) melilites, Geochimica et Cosmochimica Acta, 45, 1609-1617.

Chukanov, N.V. (2014) Infrared Spectra of Mineral Species: Extended Library. Springer-Verlag GmbH, Dordrecht–Heidelberg–New York–London, 1703 p.

Egorov L.S. (1969) Melilite rocks of the Maimecha-Kotui province. Leningrad: Nedra. 248 p..

Fleischer's Glossary of Mineral Species by Malcolm E.Back (2014) Tucson: The Mineral Record. 420 p..

Hemingway, B.S., and Robie, R.A. (1984) Heat capacity and thermodynamic functions for gehlenite and staurolite: with comments on the Schottky anomaly in the heat capacity of staurolite, American Mineralogist, 69, 307-318.

Hemingway, B.S., Evans, H.T., Nord, G.L., JR., Haselton, H.T., IR., Robie, R.A., and McGee, J.J. (1986) Ǻkermanite: phase transitions in heat capacity and thermal expansion, and revised thermodynamic data, Canadian Mineralogist, 24(3), 425-434.

Holland, T.J.B. (1989) Dependence of entropy on volume for silicate and oxide minerals: A review and a predictive model, American Mineralogist 74, 5-13.

Holland, T.J.B., and Powell, R. (1990) An enlarged an updated internally consistent thermodynamic dataset with uncertainties and correlations: the system K_2O-Na_2O-CaO-MgO-MnO-FeO-Fe_2O_3-Al_2O_3-TiO_2-SiO_2-C-H_2-O_2, Journal of Metamorphic Geology, 8, 89-124.

Holland, T.J.B., and Powell, R. (1998) An inrernally consistent thermodynamic data set for phases of petrological interest, Journal of Metamorphic Geology, 16, 309-343.

Holland, T.J.B., and Powell, R. (2011) An improved and extended inrernally consistent thermodynamic dataset for phases of petrological interest, involving a new equation of state for solids, Journal of Metamorphic Geology, 29, 333-383.

Hoschek, G. (1974) Gehlenite stability in the system CaO-Al_2O_3-SiO_2-H_2O-CO_2, Contribution in Mineralogy and Petrology,47, 245-254.

Kiseleva, I.A. (1976) Thermodynamic properties and stability of pyrope, Geochemistry International, 13,139-146.

Kiseleva, I.A., Ogorodova, L.P., Topor, N.D., and Chigareva, O.G. (1979) Thermochemical study of the CaO-MgO-SiO_2 system, Geochemistry International, 16, 122-134.

Kiseleva, I.A., Navrotsky, A., Belitsky, I.A., and Fursenko, B.A. (2001) Thermochemical study of calcium zeolites – heulandite and stilbite, American Mineralogist, 86, 448-455.

Mal'kova, M.Yu. (2006) Development of technology for building materials from blast furnace slags. Doctor dissertation. Belgorod, 422 p.

Najafinezhad, A., Abdellahi, M., Ghayour, H., Soheily, A., Chami, A., and Khandan, A. (2017) A comparative study on the synthesis mechanism, bioactivity and mechanical properties of three silicate bioceramics, Materials Science and Engineering, C 72, 259-267.

Naumov, G.B., Ryzhenko, B.N., and Khodakovskii, I.L. (1971) Reference Book of Thermodynamic Values for Geologists. Moscow Atomizdat, 239 p. (in Russian)

Navrotsky, A., and Coons, W.E. (1976) Thermochemistry of some pyroxenes and related compounds, Geochimica et Cosmochimica Acta, 40, 1281-1290.

Navrotsky, A. (2014) Progress and new directions in calorimetry: A 2014 perspective, Journal of the American Ceramic Society, 97, 3349-3359.

Neuvonen, K.J. (1952) Thermochemical investigation of the akermanite-gelenite series, Bull. Comm. Geol. Finlande, 158, 10-43.

Ogorodova, L.P., Melchakova, L.V., Kiseleva, I.A., and Belitsky, I.A. (2003) Thermochemical study of natural pollucite, Thermochimica Acta, 403, 251-256.

Ogorodova, L.P., Melchakova, L.V., Kiseleva, I.A., and Peretyazhko, I.S. (2012) Thermodynamics of natural tourmalines – dravite and schorl, Thermochimica Acta, 539, 1-6.

Ogorodova, L.P., Kiseleva, I.A., Vigasina, M.F., Kabalov, Yu.K., Grishchenko, R.O., and Melchakova, L.V. (2014) Natural sepiolite: enthalpies of dehydration, dehydroxylation, and formation derived from thermochemical studies, American Mineralogist, 99, 2369-2373.

Ogorodova, L.P., Vigasina, M.F., Melchakova, L.V., Krupskaya, V.V., and Kiseleva, I.A. (2015) Thermochemical study of natural magnesium aluminum phyllosilicate: palygorskite, Journal of the Chemical Thermodynamics, 89, 205-211.

Ottonello, G., Attene, M., Ameglio, D., Belmonte, D., Vetuschi Zuccolini, M., and Natali, M. (2013) Thermodynamic investigation of the CaO-Al_2O_3-SiO_2 system at high P and T through polymer chemistry and convex-hull techniques, Chemical Geology, 346, 81-92.

Robie, R.A., and Hemingway, B.S. (1995) Thermodynamic properties of minerals and related substances at 298.15 K and 1 bar (10^5 pascals) pressure and at higher temperatures, U.S. Geological Survey Bulletin, 2131, 461 p.

Robie, R.A., Hemingway, B.S., and Fisher, J.R. (1978) Thermodynamic properties of minerals and related substances at 298.15 K and 1 bar (10^5 pascals) pressure and at higher temperatures, U.S. Geological Survey Bulletin, 1452, 456 p.

RRUFF project. Database of Raman spectroscopy, X-ray diffraction and chemistry of minerals, http://www.rruff.info/.

Sharma, S.K., Yoder, H.S., and Matson, D.W. (1988) Raman study of some melilites in crystalline and glassy states, Geochimica et Cosmochimica Acta, 52, 1961-1967.

Shvarov Yu.V. (2008) HCh: New potentialities for the thermodynamic simulation of geochemical systems offered by Windows. Geochemistry International, 46 (8), 834-839.

Walter, L.S. (1963) Experimental study on Bowen’s decarbonation series: I: P-T univariant equilibria of the “monticellite” and “akermanite” reactions, American Journal of Science, 261, 488-500.

Weller, W.W., and Kelly, K.K. (1963) Low-temperature heat capacities and entropies at 298.15 K of akermanite, cordierite, gehlenite, and merwinite. U.S. Bureau of Mines Report Investigation, № 6343, 7 p.

Wiedenmann, D., Zaitsev, A.N., Britvin, S.N., Krivovichev, S.V., and Keller, J (2009). Alumoåkermanite, $(Ca,Na)_2(Al,Mg,Fe^{2+})(Si_2O_7)$, a new mineral from the active carbonatite-nephelinite-phonolite volcano Oldoinyo Lengai, northern Tanzania, Mineralogical Magazine, 73, 373-384.

WinX^{POW} Software Manual//STOE & CIE GmbH 2002

Xu, H., Heaney, P.J., Navrotsky, A., Topor, L., and Liu, J. (1999) Thermochemistry of stuffed quartz-derivative phases along the join $LiAlSiO_4$-SiO_2. American Mineralogist, 84, 1360-1369.

Xu, H., Navrotsky, A., Nyman, M.D., and Nenoff, T.M. (2000) Thermochemistry of microporous silicotitanate phases in the Na_2O–Cs_2O–SiO_2–TiO_2–H_2O system. Journal of Materials Research, 15, 815-823.

Xu, H., Navrotsky, A., Balmer, M.L., Su, Y., and Bitten, E.R. (2001) Energetics of substituted pollucites along the $CsAlSi_2O_6$–$CsTiSi_2O_{6.5}$ join: A high-temperature calorimetric study. Journal of the American Ceramic Society, 84, 555-560.

Figures

Figure 1. Chemical composition of studied melilites.

Figure 2. Powder XRD patterns of studied melilites.

Figure 3. Raman spectra of studied melilites.

Figure 4. FTIR spectra of studied melilites.

Figure 5. Stability fields of melilites related to contact-metamorphic reactions between calcite and silicates. Bold lines = the lower boundary of the gehlenite (1) and åkermanite (2) stability. Dotted line 3 = the lower boundary of the stability for ideal solid solution. Thin lines = the lower boundaries of the stability of studied samples in equilibrium with calcite, diopside, albite, anorthite, fayalite, wollastonite, and carbon dioxide: sample 1 – line 7, sample II – line 4, sample III – line 6, sample IV – line 5. References: circle – Walter (1963); asterisk = Hoschek (1974).

Table 1. Summary of the enthalpies of formation of åkermanite and gehlenite from the elements at T = 298.15 K (kJ/mol)

ΔH_f^0	Reference	Method of determination	ΔH_f^0	Reference	Method of determination
Åkermanite $Ca_2Mg[Si_2O_7]$			**Gehlenite $Ca_2Al[SiAlO_7]$**		
-3876.4	Neuvonen (1952)	Acid solution calorimetry	-3986.3 ± 4.0	Barany (1963)	Acid solution calorimetry
-3877.3 ± 4.2	Naumov et al. (1971)	Recalculation of data (Neuvonen 1952)	-3986.9 ± 2.9	Naumov et al. (1971)	Recalculation of data (Barany 1963)
-3876.52 ± 2.83	Robie et al. (1978)	-“-	-4007.57 ± 2.82	Robie et al. (1978)	-“-
-3866.43	Charlu et al. (1981)	Melt solution calorimetry	-3979.0	Charlu et al. (1981)	Melt solution calorimetry
-3865.1	Brousse et al. (1984)	-“-	-3988.158	Berman (1988)	Calculation from P-T equilibria
-3860.441	Berman (1988)	Calculation from P-T equilibria	-3977.26 ± 2.50	Holland and Powell (1990)	-“-
-3862.36 ± 2.61	Holland and Powell (1990)	-“-	-3985.0 ± 5.0	Robie and Hemingway (1995)	Recalculation of data (Charlu et al. 1981)
-3864.8 ± 2.0	Robie and Hemingway (1995)	Recalculation of data (Neuvonen 1952)	-3986.79 ± 2.90	Holland and Powell (1998)	Calculation from P-T equilibria
-3866.20 ± 1.06	Holland and Powell (1998)	Calculation from P-T equilibria	-3992.26 ± 1.33	Holland and Powell (2011)	-“-
-3865.63 ± 0.94	Holland and Powell (2011)	-“-	-(3969.542 – 3985.325)	Ottonello et al. (2013)	Estimation

Table 2. Chemical compositions (wt%) of studied melilites[a]

Oxides	Sample I[b] (Kovdor)	Sample II[c] (Turi Mys)	Sample III[d] (Odikhincha massif)	Sample IV[e] (Kedabek district)
Na_2O	2.57 ± 0.19	4.46 ± 0.33	4.88 ± 0.29	0.68 ± 0.08
MgO	10.20 ± 0.19	6.90 ± 0.23	6.06 ± 0.11	5.14 ± 0.07
CaO	37.18 ± 0.09	32.95 ± 0.28	32.24 ± 0.21	40.52 ± 0.31
FeO	2.42 ± 0.13	3.96 ± 0.04	4.03 ± 0.27	0.30 ± 0.41
Al_2O_3	3.81 ± 0.22	6.86 ± 0.05	7.68 ± 0.31	22.40 ± 0.76
SiO_2	44.46 ± 0.34	44.14 ± 0.86	44.71 ± 0.71	30.61 ± 0.50

[a] Uncertainties were calculated using Student's t-distribution with a 95% confidence interval; Mn, Zn, Ba, K, Ti were not detected.

[b,c,d,e] Uncertainties were calculated on the basis of seven, five, six, and five measurements, respectively.

DOI: https://doi.org/10.2138/am-2018-6475

Table 3. Unit-cell dimensions[a] and molar volumes for studied melilites[b]

Sample	a (Å)	c (Å)	V (Å^3)	$V_m^0(298.15\ K)$ (cm^3/mol)[b]
I	7.7960(4)	5.0120(5)	304.62(6)	91.72(2)
II	7.7630(4)	5.0210(5)	302.59(6)	91.11(2)
III	7.7586(4)	5.0253(5)	302.50(6)	91.08(2)
IV	7.7330(4)	5.0400(5)	301.39(6)	90.75(2)

[a] Tetragonal symmetry, space group $P\,\bar{4}2_1m$ (D^3_{2d}).

[b] Calculated using the formula: $V_m^0(298.15\ K) =$
$= a^2cN_A/Z$, where $Z = 2$, N_A = the Avogadro constant.

Table 4. Measured heats of drop solution of natural melilites in molten lead borate at 973 K*

Sample	Molar mass (g/mol)	H^0(973 K)-H^0(298.15 K) + $\Gamma_{sol}H^0$(973 K)	
		(J/g)	(kJ/mol)
$(Ca_{1.8}Na_{0.2})(Mg_{0.7}Al_{0.2}Fe^{2+}_{0.1})Si_2O_7$ (I)	272.90	853.9 ± 11.5 (6)	233.02 ± 3.14
$(Ca_{1.6}Na_{0.4})(Mg_{0.5}Al_{0.4}Fe^{2+}_{0.1})Si_2O_7$ (II)	270.02	857.7 ± 16.9 (7)	231.60 ± 4.55
$(Ca_{1.6}Na_{0.4})(Mg_{0.4}Al_{0.4}Fe^{2+}_{0.2})Si_2O_7$ (III)	273.17	846.38 ± 9.71 (7)	231.21 ± 2.65
$Ca_{2.0}(Mg_{0.4}Al_{0.6})[Si_{1.4}Al_{0.6}O_7]$ (IV)	273.57	835.5 ± 10.4 (8)	228.56 ± 2.84

* Uncertainties were calculated using Student's t-distribution with a 95% confidence interval, the number of measurements is given in parentheses.

Table 5. Thermochemical data used in calculation of the enthalpies of formation of melilites (kJ/mol)

Oxide	ΓH[a]	ΓH_f^0(298.15 K)[b]
Na_2O(s)	-111.8 ≥ 0.8[c]	-414.8 ≥ 0.3
CaO(s)	-21.78 ≥ 0.29[d]	-635.1 ≥ 0.9
MgO(periclase)	36.38 ≥ 0.59[e]	-601.6 ≥ 0.3
Fe_2O_3(hematite)	171.6 ≥ 1.9[f]	-826.2 ≥ 1.3
Al_2O_3(corundum)	107.38 ≥ 0.59[g]	-1675.7 ≥ 1.3
SiO_2(quartz)	39.43 ≥ 0.2[h]	-910.7 ≥ 1.0

[a] $\Gamma H=[H^0(973\ \mathrm{K})-H^0(298.15\ \mathrm{K})+\Gamma_{sol}H^0(973\ \mathrm{K})]$.

[b] Reference data (Robie and Hemingway 1995).

[c] According to Kiseleva et al. (2001).

[d] Calculated using $[H^0(973\ \mathrm{K})-H^0(298.15\ \mathrm{K})]$ from Robie and Hemingway (1995) and $\Gamma_{sol}H^0(973\ \mathrm{K})$ from Kiseleva et al. (1979).

[e] Calculated using $[H^0(973\ \mathrm{K})-H^0(298.15\ \mathrm{K})]$ from Robie and Hemingway (1995) and $\Gamma_{sol}H^0(973\ \mathrm{K})$ from Navrotsky and Coons (1976).

[f] Calculated using $[H^0(973\ \mathrm{K})-H^0(298.15\ \mathrm{K})]$ from Robie and Hemingway (1995) and $\Gamma_{sol}H^0(973\ \mathrm{K})$ from Kiseleva (1976).

[g] Calculated using $[H^o(973\ \mathrm{K})-H^o(298.15\ \mathrm{K})]$ from Robie and Hemingway (1995) and $\Gamma_{sol}H^o(973\ \mathrm{K})$ from Ogorodova et al. (2003).

[h] Calculated using $[H^0(973\ \mathrm{K})-H^0(298.15\ \mathrm{K})]$ from Robie and Hemingway (1995) and $\Gamma_{sol}H^0(973\ \mathrm{K})$ from Kiseleva et al. (1979).

Table 6. Thermodynamic properties at T = 298.15 K for melilites obtained in the present work[a]

Mineral	ΓH_f^0 (kJ/mol)	S^o [J/(K mol)]	ΓG_f^0 (kJ/mol)
Natural melilites			
$Ca_{1.8}Na_{0.2}(Mg_{0.7}Al_{0.2}Fe^{2+}_{0.1})Si_2O_7$ (Sample I)	-3796.3 ± 4.1	213.0 ± 0.6[b]	-3599.1 ± 4.1
$Ca_{1.6}Na_{0.4}(Mg_{0.5}Al_{0.4}Fe^{2+}_{0.1})Si_2O_7$ (Sample II)	-3753.6 ± 5.2	212.3 ± 1.3[b]	-3556.0 ± 5.2
$Ca_{1.6}Na_{0.4}(Mg_{0.4}Al_{0.4}Fe^{2+}_{0.2})Si_2O_7$ (Sample III)	-3736.4 ± 3.7	213.5 ± 1.4[b]	-3539.3 ± 3.7
$Ca_2(Mg_{0.4}Al_{0.6})[Si_{1.4}Al_{0.6}O_7]$ (Sample IV)	-3929.2 ± 3.8	213.0 ± 1.0[c]	-3731.2 ± 3.8
Melilite end members			
$Ca_2Mg[Si_2O_7]$ åkermanite Molar mass = 272.64 g/mol	-3853.9 ± 4.3[d]	212.5 ± 0.4[e]	-3656.6 ± 4.3
$Ca_2Al[SiAlO_7]$ gehlenite Molar mass = 274.20 g/mol	-3982.4 ± 3.9[f]	210. 1 ± 0.6[g]	-3782.9 ± 3.9
$CaNaAl[Si_2O_7]$ alumoåkermanite Molar mass = 258.22 g/mol	-3668.4 ± 5.1[h] -3665.5 ± 3.6[i] Average: -3667.0 ± 3.1	209.0 ± 2.8[j]	-3467.4 ± 3.2

---

[a] The uncertainties were calculated according to the law of propagation of uncertainty.
[b] Estimated using data from Hemingway et al. (1986) for åkermanite.
[c] Estimated using data from Hemingway and Robie (1984) for gehlenite.
[d] Calculated using the heat of drop solution for Sample I.
[e] From Hemingway et al. (1986).
[f] Calculated using the heat of drop solution for Sample IV.
[g] From Hemingway and Robie (1984).
[h] Calculated using the heat of drop solution for Sample II.
[i] Calculated using the heat of drop solution for Sample III.
[j] Estimated using data from (Hemingway et al. (1986) for åkermanite.

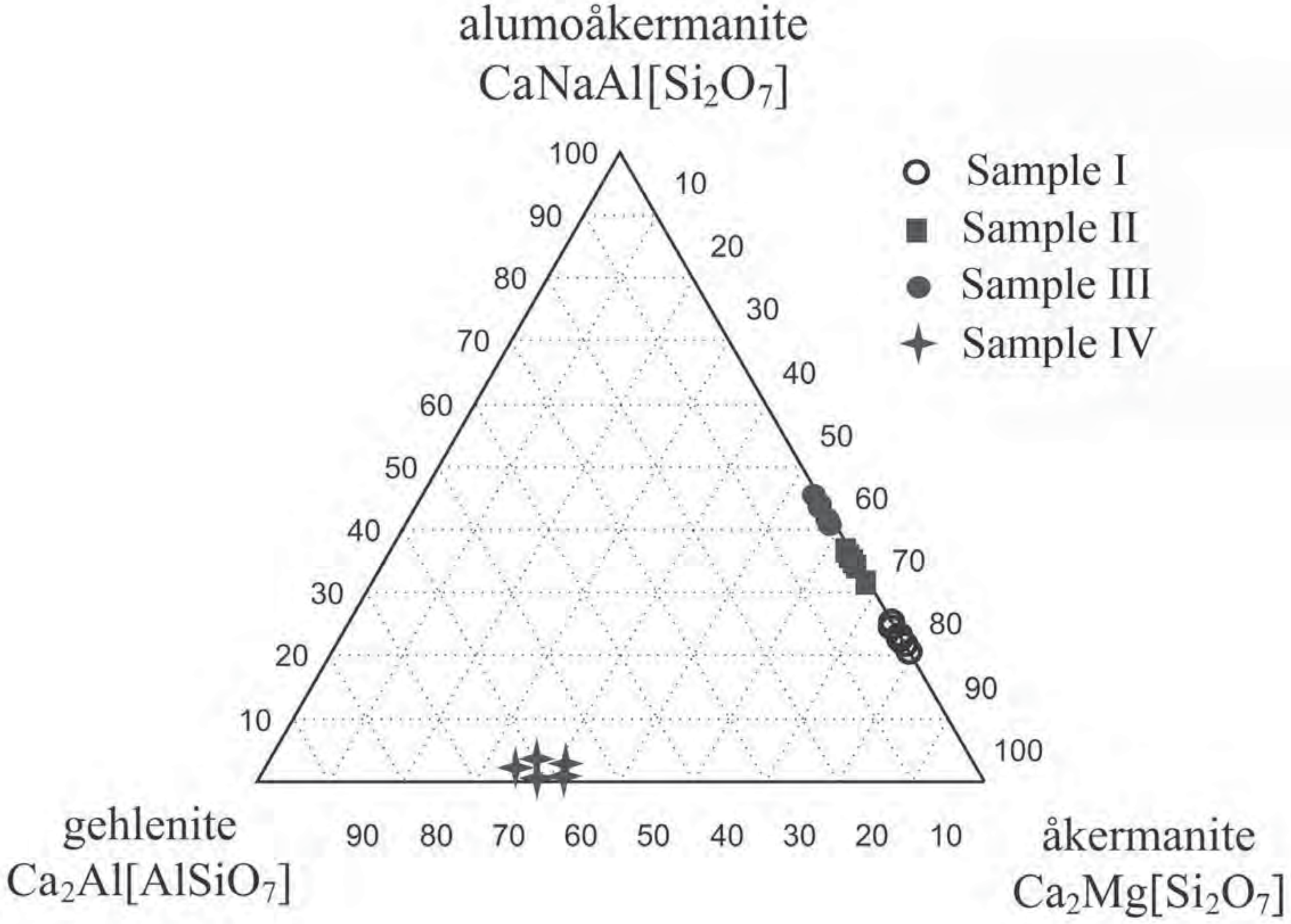
alumoåkermanite
CaNaAl[Si2O7]
gehlenite
Ca2Al[AlSiO7]
åkermanite
Ca2Mg[Si2O7]
○ Sample I
■ Sample II
● Sample III
✦ Sample IV
100
90
80
70
60
50
40
30
20
10
10
20
30
40
50
60
70
80
90
100
90
80
70
60
50
40
30
20
10

Fig. 1

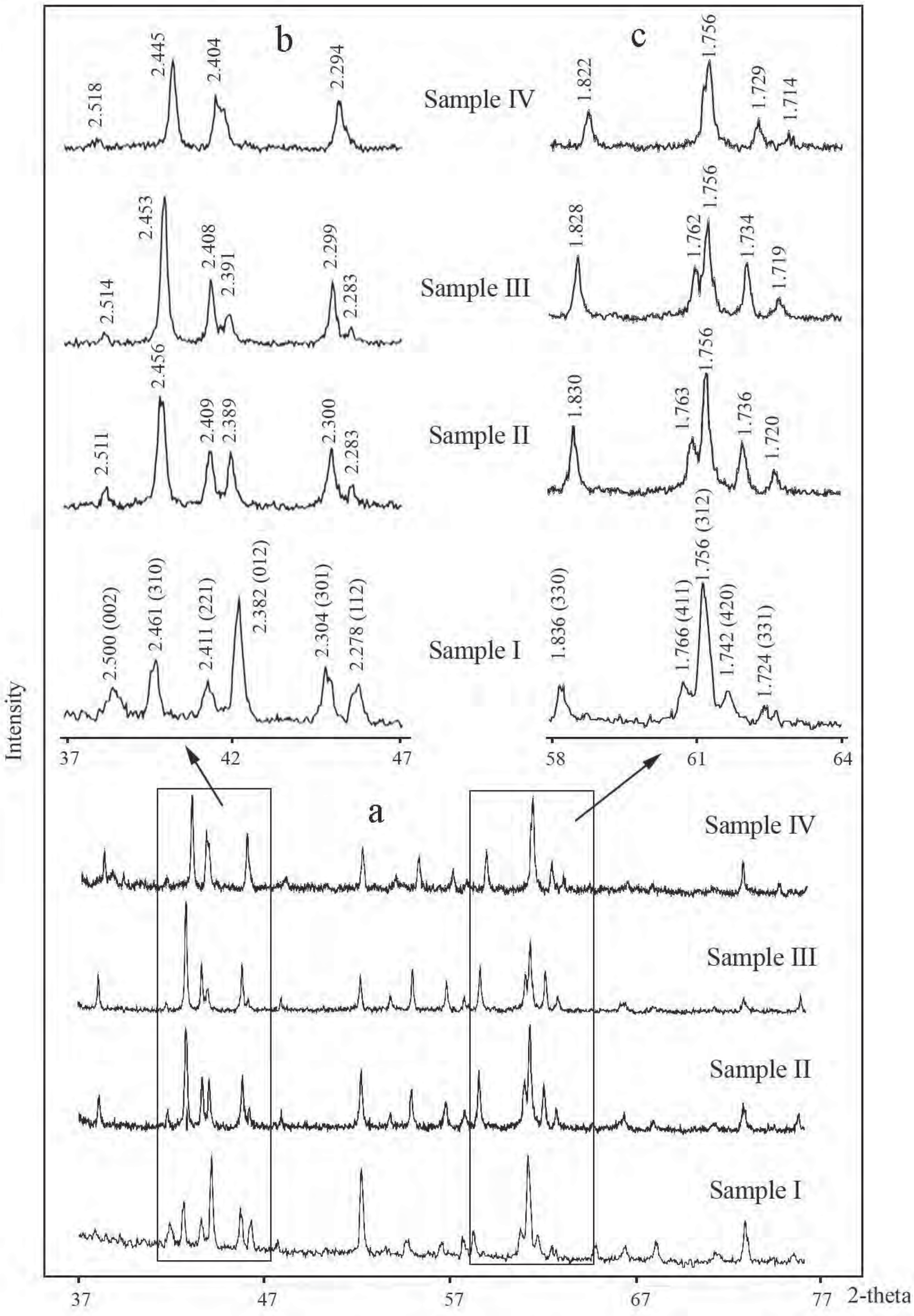
b
c
Sample IV
2.518
2.445
2.404
2.294
1.822
1.756
1.729
1.714
Sample III
2.514
2.453
2.408
2.391
2.299
2.283
1.828
1.762
1.756
1.734
1.719
Sample II
2.511
2.456
2.409
2.389
2.300
2.283
1.830
1.763
1.756
1.736
1.720
Sample I
2.500 (002)
2.461 (310)
2.411 (221)
2.382 (012)
2.304 (301)
2.278 (112)
1.836 (330)
1.766 (411)
1.756 (312)
1.742 (420)
1.724 (331)
Intensity
37
42
47
58
61
64
a
Sample IV
Sample III
Sample II
Sample I
37
47
57
67
77
2-theta

Fig. 2

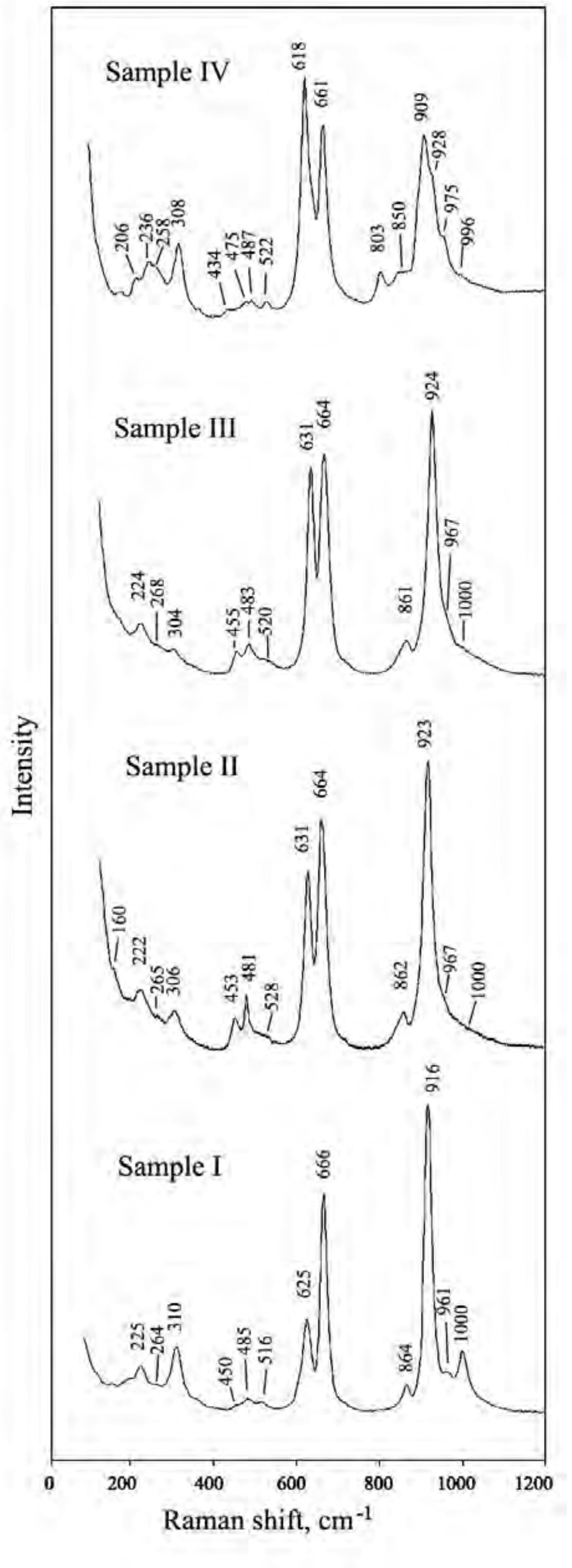
Sample IV
206
236
258
308
434
475
487
522
618
661
803
850
909
928
975
996
Sample III
224
268
304
455
483
520
631
664
861
924
967
1000
Sample II
160
222
265
306
453
481
528
631
664
862
923
967
1000
Sample I
225
264
310
450
485
516
625
666
864
916
961
1000
Intensity
0
200
400
600
800
1000
1200
Raman shift, cm-1

Fig. 3

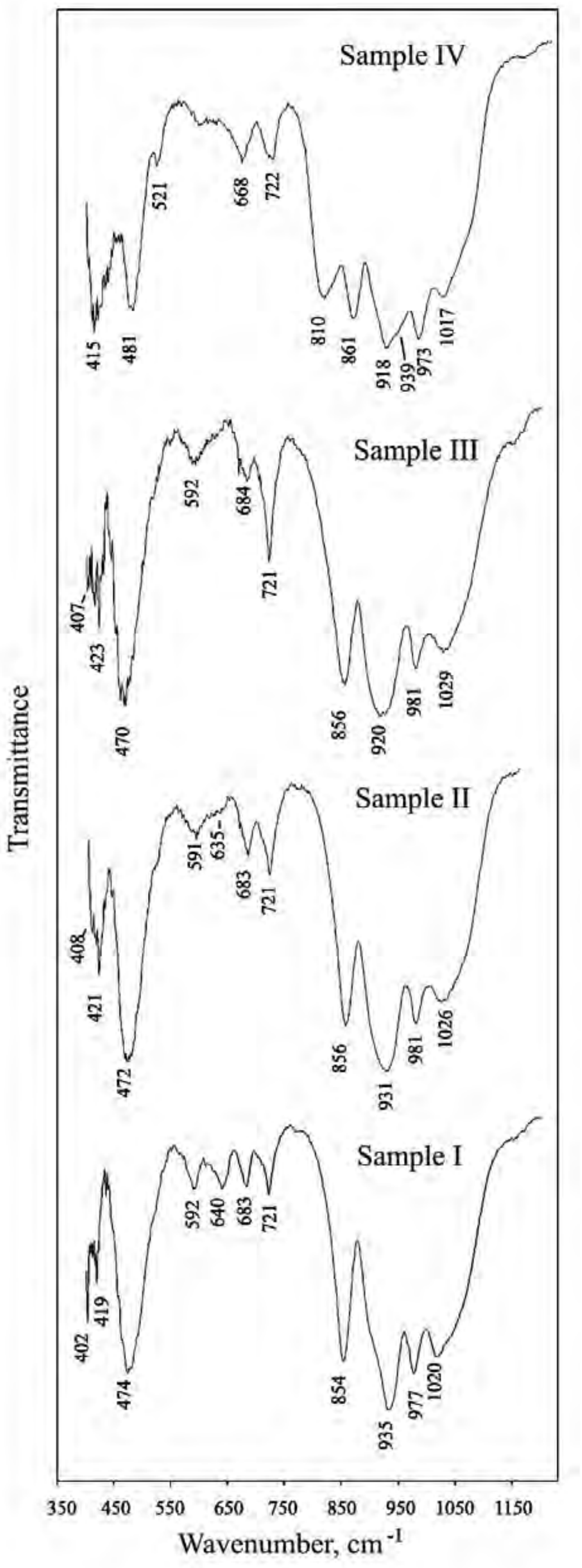
Sample IV
415
481
521
668
722
810
861
918
939
973
1017
Sample III
407
423
470
592
684
721
856
920
981
1029
Sample II
408
421
472
591
635
683
721
856
931
981
1026
Sample I
402
419
474
592
640
683
721
854
935
977
1020
Transmittance
350
450
550
650
750
850
950
1050
1150
Wavenumber, cm⁻¹

Fig. 4

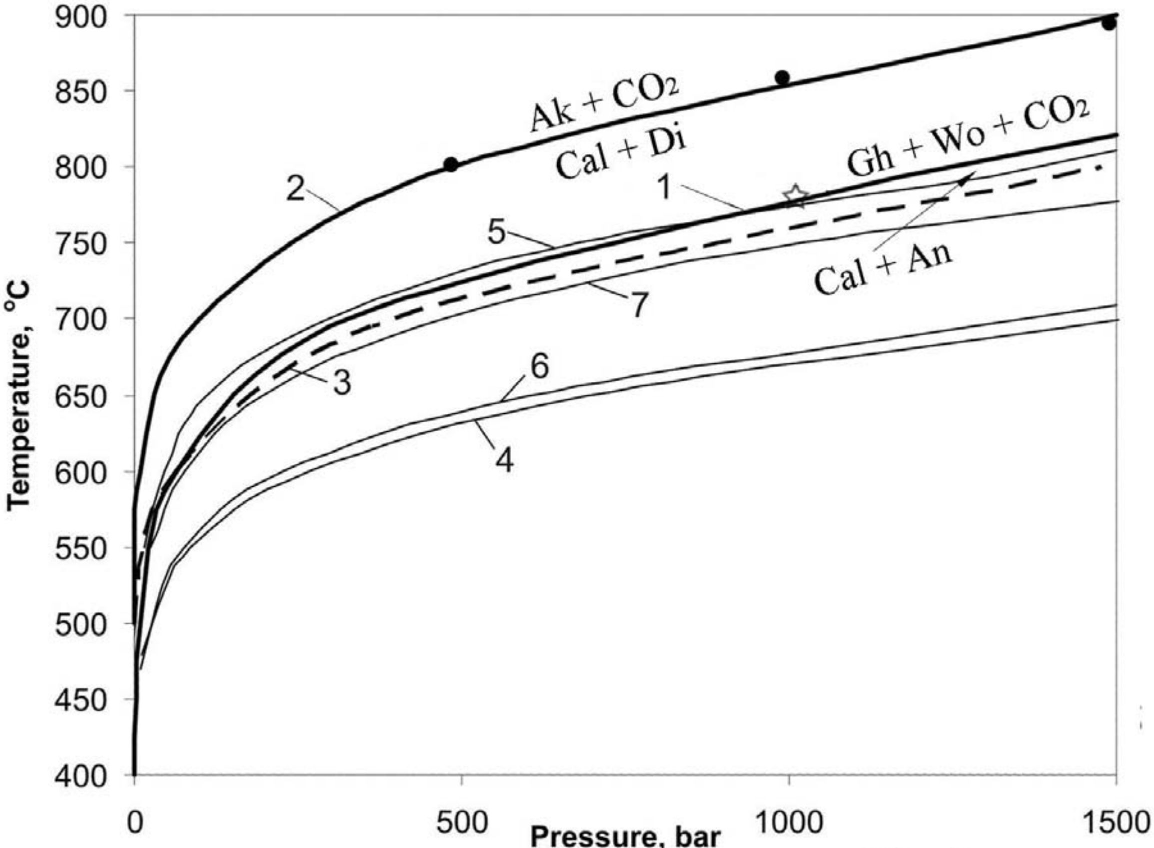
900
850
800
750
700
650
600
550
500
450
400
Temperature, °C
0
500
1000
1500
Pressure, bar
Ak + CO2
Cal + Di
Gh + Wo + CO2
Cal + An
1
2
3
4
5
6
7

Fig. 5